

AperTO - Archivio Istituzionale Open Access dell'Università di Torino

Exploring Synthetic Pathways to Cationic Heteroleptic Cyclometalated Iridium Complexes Derived from Dipyridylketone

This is the author's manuscript

Original Citation:

Availability:

This version is available <http://hdl.handle.net/2318/113715> since

Published version:

DOI:10.1039/c2dt30399j

Terms of use:

Open Access

Anyone can freely access the full text of works made available as "Open Access". Works made available under a Creative Commons license can be used according to the terms and conditions of said license. Use of all other works requires consent of the right holder (author or publisher) if not exempted from copyright protection by the applicable law.

(Article begins on next page)



UNIVERSITÀ DEGLI STUDI DI TORINO

This is an author version of the contribution published on:

Questa è la versione dell'autore dell'opera:

Dalton Transactions, 41, 2012, 10.1039/c2dt30399j

The definitive version is available at:

La versione definitiva è disponibile alla URL:

<http://pubs.rsc.org/en/Content/ArticleLanding/2012/DT/c2dt30399j>

Exploring Synthetic Pathways to Cationic Heteroleptic Cyclometalated Iridium Complexes Derived from Dipyritylketone

Giorgio Volpi, Claudio Garino and Carlo Nervi*

Dipartimento di Chimica, Università di Torino, Via P. Giuria n° 7, I-10125 Torino (Italy)

Abstract

Reactions between 2,2'-dipyritylketone (**L1**) and different amines gave a series of iminic ligands, and their chemical reductions produced the related amines. The organic ligands have been employed in the syntheses of the corresponding new phosphorescent six-member ring bis-cyclometalated heteroleptic iridium(III) complexes of general formula $[\text{Ir}(\text{ppy})_2(\text{L})]^+$, (ppy=2-phenylpyridine), namely **IrLn**. The metal complexes containing *N*-(dipyridin-2-ylmethylene)butan-1-amine (**IrL2**), *N*-(dipyridin-2-ylmethyl)butan-1-amine (**IrL5**), *N*-(dipyridin-2-ylmethyl)butane-1,4-diamine with amino groups protected by Boc (**IrL6-Boc**) and TFA (**IrL6-TFA**), and *N*-(dipyridin-2-ylmethyl)-*N*-methylbutan-1-amine (**IrL8**) have been characterized and their electronic and spectroscopic properties interpreted by DFT calculations. Organoiridium complexes containing amines and imines were found to have high and low photoemission quantum yields, respectively, and their features rationalized by quantum mechanic calculations. Some of these complexes show reasonable quantum yields (up to 13%), long lifetime (up to 2.3 μs) and high stability. Complementary and alternative synthetic pathways to get cationic heteroleptic cyclometalated Ir complexes bearing a tethered primary amino group have been explored with the aim to obtain organometallic phosphorescent derivatives suitable for surface functionalization.

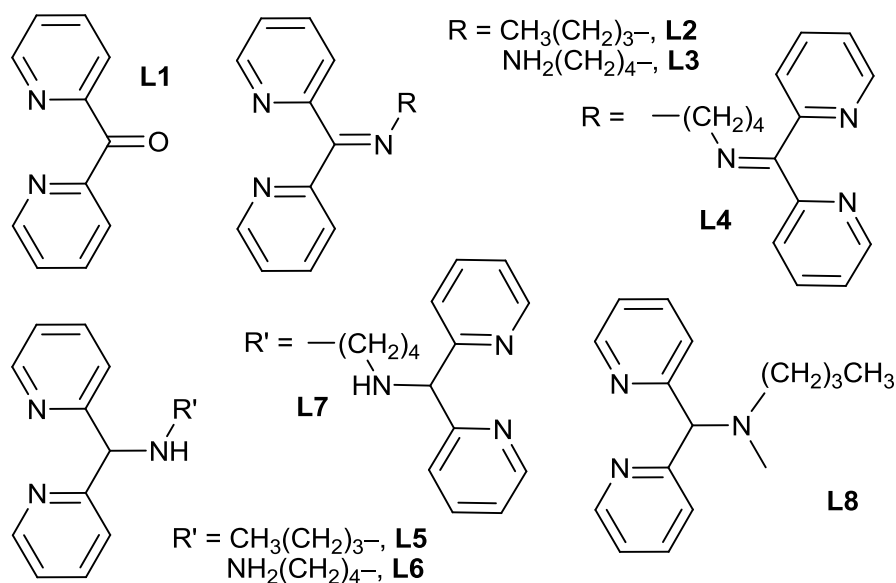
* Corresponding author. E-mail: carlo.nervi@unito.it

Introduction

Among the plethora of transition metal complexes owing to excellent photophysical properties, cyclometalated iridium(III) complexes play an important role because of their high emission quantum yields, long lifetimes, high thermal- and photo-stabilities, and also because the emission in the visible can be tuned to cover the range of colours from blue to red.¹⁻⁵ Good solubility for solution-processable light-emitting devices is another desirable feature for this class of complexes.^{3,6} The interest in cyclometalated Ir(III) complexes is continuously renewed and alternative synthetic procedures that lead to products incorporating functional group capable to improve the desired feature (for example solubility) remains of high importance. These class of complexes are typically sensible to molecular oxygen,⁷ so that emission of light from aerated solutions is strongly quenched. One of the reasons of this negative aspect finds its origin in the long lifetimes of the triplet metal-to-ligand charge transfer (³MLCT) states, which makes the metallic complexes sensible to the electron transfer reaction.⁸ This characteristic is commonly seen in ³MLCT of transition metal complexes, especially when ³MLCT is structurally exposed to external contacts with other molecules. It has been tentatively diminished adopting Ir-caged complexes,⁹ but in other cases it can be turned into a desirable feature. For example, in photodynamic therapy (PDT) Ru porphyrine¹⁰ and Ir complexes¹¹ have been used as singlet oxygen makers. Very recently¹² it was pointed out that Ir cyclometalated complexes show high near-infrared two-photon absorption, a highly-desired feature for *in vivo* high resolution PDT with good tissue penetration. Photoemission quenching of photo-sensitizers is also the basis of “artificial photosynthesis” in carbon dioxide reduction¹³ and hydrogen production. Ru derivatives¹⁴ and Ir bis-cyclometalated¹⁵⁻¹⁹ complexes have been employed to produce H₂ from formic acid and water, respectively. In water-splitting reaction the [Ru(bpy)₃]⁺-type complexes have been historically the most common photo-sensitizers choice, but Ir(III) derivatives have come under investigation as superior alternatives.¹⁷

Lately we studied the complex [Ir(ppy)₂(2,2'-dipyridylketone)]⁺ (**IrL1**)²⁰ and exploited its reactivity to get new Ir complexes pinched by a N-N six-member ring, characterized by relatively high photoemission quantum yields.²¹

The aim of the present paper is to illustrate new synthetic attempts in trying to get luminescent Ir derivatives by taking advantage of the **L1** reactivity (Scheme 1). We used the classical reaction between ketone and amine that give Schiff bases,²²⁻²⁵ following similar synthetic strategy to that developed for Ir bis-cyclometalated derivatives.^{20,21} Several new cationic heteroleptic cyclometalated iridium complexes has been synthesized and characterized by NMR, fluorescence spectroscopy and electrochemical techniques.



Scheme 1. Sketch of the synthesized ligands aiming to obtain the corresponding cationic heteroleptic bis-cyclometalated Ir complexes

Furthermore, functionalization of surfaces is attracting interest because applications as sensors, molecular electronics, analytical detections, and catalysis.²⁶⁻³¹ There are several examples of molecules covalently bonded on solid surface, but few cases make use of clean organometallic complexes. We recently show an electrochemical synthetic strategy which allows to link an intact organometallic complex on a carbon solid surface *via* a covalent bond.³¹ The procedure requires the presence of an electro-oxidable amino group on the ancillary ligand of the organometallic complex. With respect to this goal, and by using the same methodological approach, we herein also explored the synthetic pathways to get cationic heteroleptic cyclometalated Ir complexes bearing a tethered primary amino group suitable for surface functionalization.

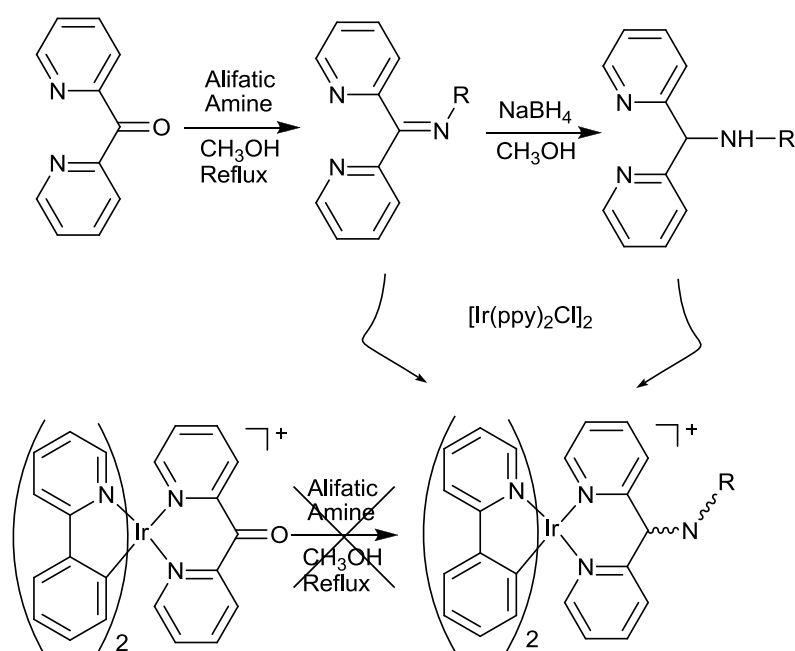
Results and discussion

Syntheses of imine and amine derivatives

The standard synthesis of these class of Ir complexes is based on the direct reaction of the dimer $[\text{Ir}(\text{ppy})_2(\mu\text{-Cl})_2]$ with N,N' dipyridyl molecules giving Cl^- as counterion. However, when the employed ligand contains a potentially coordinating group (like a terminal amino group), the synthesis could give rise to several side reaction products with low reaction yields. To circumvent the problem we reported a new synthetic procedure²¹ involving first the reaction of 2,2'-dipyridylketone (**L1**) with the dimer $[\text{Ir}(\text{ppy})_2\text{Cl}]_2$ that easily affords the complex **IrL1** (having low emission quantum yield) as pure product in good yield (91%);²⁰ then the reactivity of the carbonyl moiety in **IrL1** is used to get several derivatives with higher emission quantum yields.

The imine ligands **L2-L4** (Scheme 1) were synthesized by direct reaction of **L1** with the appropriate amine. Ketones are less reactive than aldehydes in the formation of Schiff bases, and reactions involving aromatic rings, as in 2,2'-dipyridylketone, require much more vigorous conditions.²² Refluxing methanol assisted the reaction of amines with **L1** by water removal, but, interestingly, the reaction carried on **IrL1** in identical conditions did not proceed at all.

Butyl amine reacts with **L1** giving the Schiff base **L2** that in turn reacts with $[\text{Ir}(\text{ppy})_2\text{Cl}]_2$ affording **IrL2** complex in good yield. Probably in **L2** the imino group is sufficiently hindered to the metal coordination by the alkyl chain. Imine **L2** can be easily reduced to the corresponding saturated counterpart **L5** (Scheme 2). Treatment of **L5** with methyl iodide gave the tertiary amine **L8**. It is interesting to note that also in this case **IrL5** did not react with methyl iodide, so that **IrL8** can be obtained only by the reaction of the methylated ligand **L8** with the Ir dimer.



Scheme 2: Sketch of the syntheses of **IrL_n** complexes.

Whereas strong interferences in the reactions between the precursor Ir dimer and the reduced forms of **L1** carrying groups like –OH, –CN and =N–NH₂ prevent the syntheses of iridium derivatives,²¹ the opposite situation is herein observed (Scheme 2). This behaviour is difficult to rationalize, but it can probably be ascribed to steric and electronic properties. It is worth noting that in all the present cases only the two nitrogen atoms of the bipyridine coordinate the metal, similar to what is observed for other metal complexes.^{32,33}

The use of alkyl diamine in the reaction with **L1** could lead to a ligand containing a hanging primary amino group suitable for surface functionalization, or to a dimeric-type ligand, depending on the relative molar ratio employed. Dinuclear symmetric complexes of the type M–L–M with equivalent metal centres have been studied for their applications in photochemical induced electron transfer,^{34,35} mixed-valence complexes,³⁶ and material for molecular devices.^{37,38} By using putrescine:2,2'-dipyridylketone in molar excess and 1:2 stoichiometric ratio instead of butylamine, the imine ligands **L3** and **L4** were obtained, respectively. Their chemical reduction resulted in the corresponding amines **L6** and **L7**. The dimeric ligands **L4** and **L7**, containing six potential coordinating sites, in the early stage of the reaction apparently gave the corresponding complexes **IrL4** and **IrL7**, but they shown to be unstable, restoring **IrL1** (isolated from the reaction mixture) by quick degradation. This observation gives hints for understanding why **IrL1** is reluctant to react with amines. The corresponding free ligands have been shown to be slightly unstable too,³⁹ and the coordination to the metal very probably enhances this instability. These negative results are in agreement with similar works that include a class of chelating ligands containing two 2-pyridyl substituents spaced by a single atom.⁴⁰⁻⁴² Besides, it is not surprising that the ligands **L3** and **L6** containing a pendent –NH₂ gave several side-reaction products, difficult to separate, and with very low reaction yields.

With the aim to get an organometallic Ir(III) cyclometalated derivative with an aliphatic primary amino group ready to be employed for functionalization of carbon surfaces, we thought to lock the –NH₂ reactivity of **L6** by the classical organic reversible protection groups. We used *N*-tert-butyloxycarbonyl (Boc), fluorenylmethyloxycarbonyl (Fmoc) and trifluoroacetyl (TFA) groups,^{24,43-51} and subsequently proceeded to the complexation reaction with the metal. For all the three protecting groups, **L6** readily reacts at both primary and secondary amine sites. Upon reaction with [Ir(ppy)₂Cl]₂, **L6-Fmoc** unluckily gave a multitude of side products difficult to separate and no **IrL6-Fmoc** has been obtained. Conversely, **IrL6-Boc** and **IrL6-TFA** were separated with good (68.5%) and moderate (35.0%) yields, respectively. Unfortunately, the removal of protective groups from **IrL6-Boc** and **IrL6-TFA** in acidic (TFA/CH₂Cl₂) and basic (MeOH/Na₂CO₃) conditions, respectively, resulted in a complete degradation of the metal complexes.

Computed geometries and electronic structures

Singlet ground state (S₀) geometries of the complexes **IrL2**, **IrL5**, **IrL6** and **IrL8** were optimized in the gas phase using the B3LYP method (**Error! Reference source not found.**). Calculations on **IrL6** are extrapolated to the complexes with

Table 1. Selected bond lengths [Å] and angles (°) of **IrL1**, **IrL2**, **IrL5**, **IrL6** and **IrL8** on calculated ground state (S₀) and lowest-lying triplet state (T₁) geometries, and X-ray crystallography. Nitrogen atoms N1 and N2 belongs to the two ppy ligands, whereas N3 and N4 belongs to the L ligands

Complex		Ir–N1	Ir–C1	Ir–N2	Ir–C2	Ir–N3	Ir–N4	N1–Ir–C1	N2–Ir–C2	N3–Ir–N4
IrL1 ^{19,20}	X-ray	2.039	2.007	2.041	2.015	2.179	2.153	80.45	80.96	86.96
	S ₀	2.090	2.024	2.085	2.023	2.264	2.249	79.99	80.12	85.67
	T ₁	2.093	2.005	2.082	1.997	2.243	2.209	80.65	80.67	83.32
IrL2	S ₀	2.087	2.023	2.091	2.023	2.265	2.270	79.96	80.00	85.46
	T ₁	2.085	2.025	2.082	2.024	2.248	2.257	79.98	80.15	85.86
IrL5	S ₀	2.085	2.020	2.097	2.021	2.297	2.322	79.95	80.09	85.03
	T ₁	2.101	2.105	2.070	1.980	2.338	2.347	80.00	81.80	83.95
IrL6	S ₀	2.086	2.019	2.096	2.021	2.297	2.323	79.94	80.09	85.07
	T ₁	2.055	1.979	2.014	2.113	2.317	2.368	81.65	80.12	83.92
IrL8	S ₀	2.086	2.016	2.101	2.019	2.320	2.334	79.95	80.01	84.44
	T ₁	2.103	2.012	2.071	1.977	2.369	2.358	79.99	81.75	83.47

pending –NH₂ protected, namely **IrL6-Boc** and **IrL6-TFA**. This approximation seems reasonable and

supported by the very similar spectroscopic features of the two complexes. We were unable to get suitable crystals for X-ray diffraction analysis. However, bond lengths and angles are similar to those of **IrL1**, which are in excellent agreement with the experimental data. All the complexes have a pseudo-octahedral coordination structure; the Ir–N(ppy), Ir–C(ppy), and Ir–N(L) bond lengths are in the range 2.085–2.101, 2.016–2.024, and 2.249–2.334 Å, respectively. In all optimized geometries, N–Ir–C and N–Ir–N angles are found to be very similar. The bite angle of the ppy ligands (N1–Ir–C1 and N2–Ir–C2) is relatively small, close to 80°, whereas the bite angle of the L ligands (N3–Ir–N4) spans from 84.44° to 85.67°. The main geometrical parameters of **IrL2**, **IrL5**, **IrL6** and **IrL8** in the lowest-lying triplet state (T_1) are also shown in **Error! Reference source not found.** Compared to the data of the ground state, there are some variations. In particular, the Ir–N3/N4 bond lengths are shortened in **IrL2** (by 0.017 and 0.013 Å) and lengthened in **IrL5** (by 0.041 and 0.025 Å), **IrL6** (by 0.020 and 0.045 Å), and **IrL8** (by 0.049 and 0.024 Å). A specific trend is not observed in the case of the Ir–C1/C2 and Ir–N1/N2 bond lengths of those complexes, while it is worth noting that the C=N double bond of the **IrL2** triplet state is significantly lengthened (0.113 Å). The same phenomena is observed in **IrL1** (C=O double bond of **L1**) and in $[\text{Ir}(\text{ppy})_2(2,2' \text{-}(\text{hydrazonomethylene})\text{dipyridine})]^+$ (C=N double bond of the organic ligand), being 0.045 Å and 0.106 Å longer in the triplet state with respect to the ground state, respectively.²¹ This is in agreement with the population of excited states with antibonding features along the C=O and the C=N bonds of these compounds, and fits very well with the analogy between excited- and reduced-states.⁵²

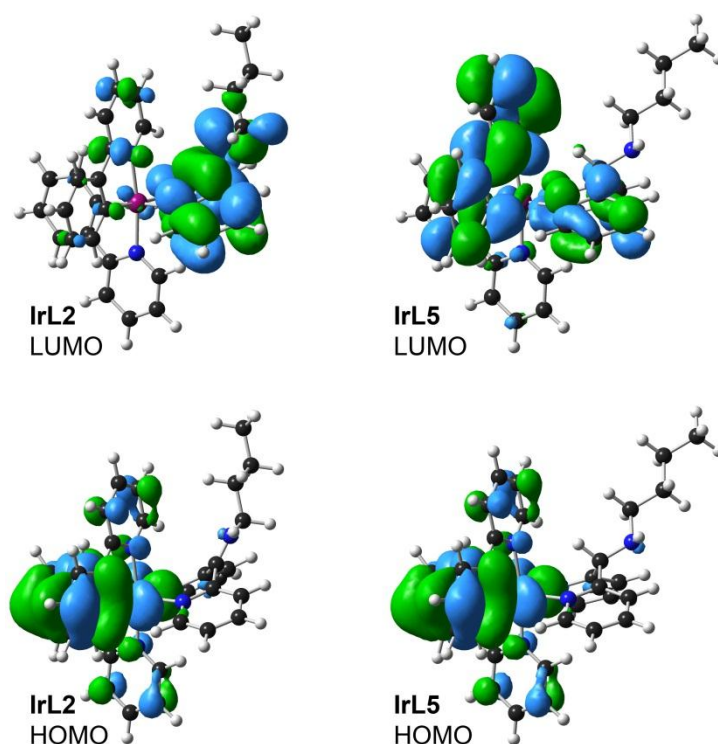


Figure 1. Frontier orbitals for complexes **IrL2** and **IrL5**.

To provide insight into the electronic structure of **IrL2**, **IrL5**, **IrL6** and **IrL8**, we performed single-point calculations on the optimized geometries, taking into account the solvent effect (acetonitrile). The complexes have common orbital features. For all complexes, the highest occupied molecular orbital (HOMO) is a combination of Ir(d) and ppy(π) orbitals, centred on the Ir atom and on the two phenyl groups of the ppy ligands (Figure 1 and ESI). The HOMO is followed, at lower energy (to less than 0.5–0.6 eV below), by five, six, or seven combinations of Ir(d) and ppy and/or L(π) orbitals. These orbitals are very close in energy (within 0.454–0.482 eV) and are followed by the π -bonding framework of the L ligand (to less than 0.5–0.6 eV below). The lowest unoccupied molecular orbitals (LUMOs) of **IrL2**, **IrL5**, **IrL6** and **IrL8** are preferentially localized on the ligands. The LUMOs of **IrL5**, **IrL6** and **IrL8** are π^* orbital delocalized on

one ppy and on the aromatic rings of **L**, with no contribution from the aliphatic portion. Conversely, the **IrL2** LUMO is a π^* orbital localized on the whole **L2**, with relevant antibonding features along the C=N double bond. An analogue situation was observed in the cases of **IrL1** and [Ir(2-phenylpyridine)₂(2,2'-(hydrazonomethylene)dipyridine)]⁺, the LUMOs of which are π^* orbitals localized on the whole ancillary ligands with antibonding character. The contribution of the singlet–triplet transitions that features along the C=O and C=N double bonds, respectively.²¹

For all complexes, the LUMOs are followed in energy by a series of ppy and **L** π^* orbitals.

Photophysical properties

Electronic absorption spectra of **IrL2**, **IrL5**, **IrL6-Boc**, **IrL6-TFA** and **IrL8** were recorded at room temperature in acetonitrile solutions. Results are summarized in **Error! Reference source not found.**. Typical Ir(III) complexes have a multitude of concurrent electronic transitions, involving singlet and triplet metal-to-ligand charge-transfer (¹MLCT and ³MLCT) transitions, and singlet and triplet ligand-centered (¹LC and ³LC) transitions. Moreover, intraligand charge-transfer (ILCT) and ligand-to-ligand charge-transfer (LLCT) should be considered, depending on the coordinated ligands.

Table 2. Absorption and emission data for complexes **IrL1**, **IrL2**, **IrL5**, **IrL6-Boc**, **IrL6-TFA** and **IrL8** in deaerated acetonitrile solutions

Complex	$\lambda_{\text{abs}}/\text{nm}$	$\lambda_{\text{em}}/\text{nm}$	Φ	$\tau_{\text{av}}/\mu\text{s}$
IrL1	262	(678)	<0.005	–
	288 ^a			
	333 ^a			
	376			
	480			
IrL2	262	453	<0.005	–
	337 ^a	480		
	376	530		
	490			
IrL5	258	487	0.13	1.662
	295 ^a	513		
	342	549		
	388			
	422			
IrL6-Boc/	262/258	478/488	0.04/0.09	0.215/0.59
IrL6-TFA	306 ^a /306 ^a	506/511		
	340 ^a /340 ^a	540/450		
	378/378			
	410/425			
IrL8	258	480	0.10	2.311
	306 ^a	507		
	330 ^a	541		
	380			
	460			

^a Shoulders

The complexes **IrL2**, **IrL5**, **IrL6-Boc**, **IrL6-TFA** and **IrL8** show intense absorption bands in the range 250–300 nm, less intense features in the range 300–400 nm with tails which extend into the visible region, and no absorption above 500 nm.

The nature of the electronic transitions responsible for the absorption bands was elucidated using TD-DFT calculations. Sixty-four singlet and eight triplet excited states were computed starting from the gas-phase optimized geometry. The solvent effect was taken into account by using the CPCM method. The high-energy absorptions are well described by TD-DFT, but for these Ir systems the spin-orbit coupling makes possible to experimentally observe the normally forbidden singlet–triplet absorptions.⁵³ Triplet excited states were calculated in order to dominate the low-energy portion of the spectra, due to the efficient spin orbit coupling.

Since the TD-DFT calculation used here neglect the spin-orbit coupling, the singlet–triplet transitions have zero oscillator strength and in Figure 2 they are drawn with arbitrary intensity.

The absorption spectrum of **IrL1** shows an intense UV band at $\lambda = 262$ nm, and can be ascribed to mixed $^1\text{LC}/^1\text{MLCT}$ transitions involving all ligands (**L1** is the unit receiving electron density). A second band (shoulder) at $\lambda = 376$ nm is assigned to Ir-ppy \rightarrow ppy singlet transitions. According to calculations, the broad and weak absorption band of **IrL1** at $\lambda = 480$ nm is a singlet Ir-ppy \rightarrow **L1** transition.

The complex **IrL2** has an absorption band centred at $\lambda = 262$ nm due to mixed $^1\text{LC}/^1\text{MLCT}$ transitions involving all ligands (**L2** is the unit receiving electron density). The shoulder at $\lambda = 337$ nm is a Ir-ppy \rightarrow **L2** transition, while the feature at 376 nm can be assigned to two transitions (Ir-ppy \rightarrow ppy and Ir-ppy \rightarrow **L2**) having mixed $^1\text{LC}/^1\text{MLCT}$ character. The weak band experimentally found at 490 nm can be related to the presence of two singlet–triplet transitions having a mixed $^3\text{LC}/^3\text{MLCT}$ character (Ir-ppy \rightarrow ppy at 447 nm, Ir-ppy \rightarrow **L2** at 460 nm).

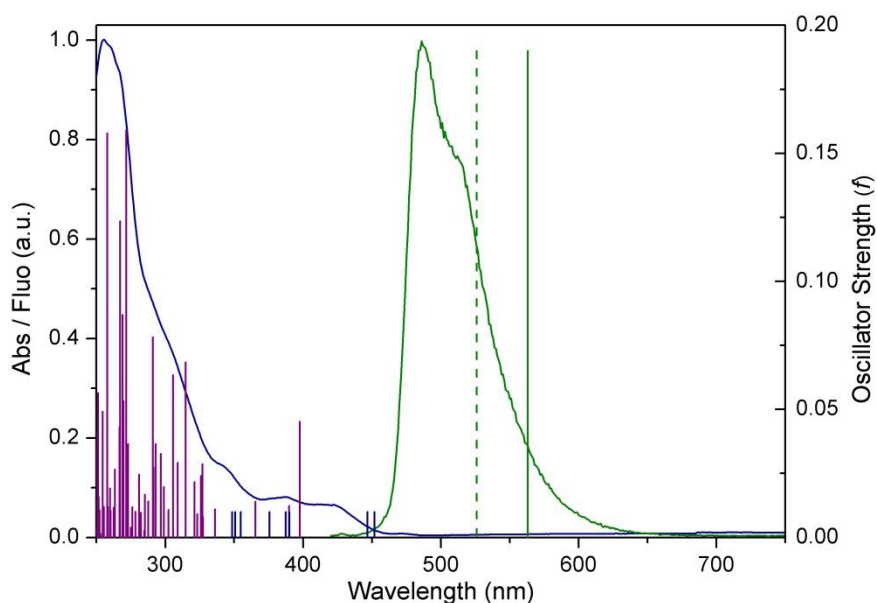


Figure 2. Experimental absorption (blue line) and emission (green line) spectra, calculated singlet (purple bars) and triplet (blue bars) excited state transitions, and estimated emission energy using ΔSCF (dashed green bar) and TD-DFT (solid green bar) approaches, of complex **IrL5** in acetonitrile. The vertical bar heights of singlet transitions are equal to the oscillator strengths, while the other bars have arbitrary intensities.

In the case of **IrL5**, calculations attribute the UV band at $\lambda = 258$ nm to mixed $^1\text{LC}/^1\text{MLCT}$ transitions involving all ligands (**L5** is now the unit receiving electron density). The shoulder falling at $\lambda = 295$ nm can be ascribed to Ir-ppy \rightarrow ppy-**L5** absorption. The less intense band at 342 nm is due to mixed $^1\text{LC}/^1\text{MLCT}$ (Ir-ppy \rightarrow **L5**) transitions, while the one at $\lambda = 388$ nm is due to Ir-ppy \rightarrow ppy contribution. The band experimentally found at 422 nm can be related to three singlet–triplet absorptions having mixed $^3\text{LC}/^3\text{MLCT}$ character (Ir-ppy \rightarrow ppy at 447 nm and Ir-ppy \rightarrow ppy-**L3** at 452 nm), and the very weak band at *ca.* 475 nm can be due to a singlet–triplet transition.

The absorption spectrum of **IrL6-Boc** and **IrL6-TFA** show an intense UV band at $\lambda = 262$ and 258 nm, respectively, that can be ascribed to mixed $^1\text{LC}/^1\text{MLCT}$ transitions involving all ligands (**L6** is the unit receiving electron density). The shoulder at $\lambda = 306$ nm is due to Ir-ppy \rightarrow ppy-**L6** and Ir-ppy \rightarrow ppy transitions, while the one at $\lambda = 340$ nm can be related to an Ir-ppy \rightarrow **L6** transition. Calculations on **IrL6** attribute the less intense band at 378 nm to Ir-ppy \rightarrow ppy transitions, having a mixed $^1\text{LC}/^1\text{MLCT}$ character, while the tail at 410/425 nm is ascribed to two singlet–triplet absorptions (447 and 452 nm) having mixed $^3\text{LC}/^3\text{MLCT}$ character Ir-ppy \rightarrow ppy-**L6**.

Finally, **IrL8** displays an intense band at $\lambda = 258$ nm that can be ascribed to mixed $^1\text{LC}/^1\text{MLCT}$ transitions involving all ligands (**L8** is the unit receiving electron density). The two shoulders at $\lambda = 306$ nm and $\lambda = 330$ nm are essentially due to Ir-ppy \rightarrow ppy-**L8** transitions, and in the case of the second shoulder a Ir-ppy \rightarrow ppy

transition is also contributing. The less intense feature at 380 nm can be ascribed to two transitions having a mixed $^1\text{LC}/^1\text{MLCT}$ character (Ir-ppy \rightarrow ppy-**L8** and Ir-ppy \rightarrow ppy). The weak band experimentally found at 460 nm can be related to a singlet–triplet transition having a mixed $^3\text{LC}/^3\text{MLCT}$ character (Ir-ppy \rightarrow ppy-**L8** transition at 448 nm).

When excited in acetonitrile solution at room temperature, all complexes show luminescence properties strongly dependent on oxygen quenching. **IrL2** is a very weak emitter, showing a structured emission with maxima at 453, 480 and 530 nm and an emission quantum yield lower than 0.005. On the contrary, **IrL5**, **IrL6-Boc**, **IrL6-TFA** and **IrL8** exhibit intense emission spectra with prominent vibronic structures and several maxima, reasonable high quantum yields ($\Phi = 0.13, 0.04, 0.09$ and 0.10) and relatively long excited state lifetimes ($\tau = 1.662, 0.215, 0.591$ and $2.311 \mu\text{s}$), respectively.

The lowest triplet state, which is responsible for phosphorescence emission, can be either $^3\text{MLCT}$ or ^3LC and is generally accepted to describe the emitting state as a mix of MLCT and LC excited states.⁵⁴ The emission lifetimes and the effective quenching by oxygen molecules of the luminescence quantum yields are indicative of emission properties due to triplet excited states. In terms of spectral shape, with the exception of **IrL2** (see below), we can attribute the emission of **IrL5**, **IrL6** and **IrL8** to structured LC phosphorescence.

To gain insight into the nature of the excited states involved in the emission process, we used two different computational approaches. The first consisted on TD-DFT calculations of triplet excited states from the ground state, using the lowest-lying triplet state geometries, the second employed the DFT/UKS calculation (unrestricted Kohn–Sham) of lowest-lying triplet geometries (ΔSCF method, see the Computational details). ΔSCF gives satisfactory results, predicting the emission of **IrL5** at 526 nm (experimental 487 nm), the emission of **IrL6** at 529 nm (experimental 487/488 nm), and the emission of **IrL8** at 527 nm (experimental 480 nm). Contrariwise, TD-DFT underestimates the emission energy of **IrL5**, **IrL6** and **IrL8** (calculated 563 nm, 567 nm, 563 nm). According to triplet excited state calculations obtained by TD-DFT, for **IrL5** and **IrL8** the luminescence is due to a mixed $^3\text{LC}/^3\text{MLCT}$ (Ir-ppy \rightarrow ppy) emissive state (**Error! Reference source not found.**), confirmed by the spin density of the lowest-lying triplet-state obtained with the unrestricted Kohn–Sham formalism (**Error! Reference source not found.** and Fig. ESI5). These calculations applied to **IrL2** only apparently give similar results (see below). The very weak emission of **IrL2** can apparently be ascribed to a triplet–singlet transition involving the double C=N bond of **L2**. Both the lowest singlet and triplet absorptions have mixed LC/MLCT character involving the population of the LUMO (π^* orbital localized on the **L2** ligand).

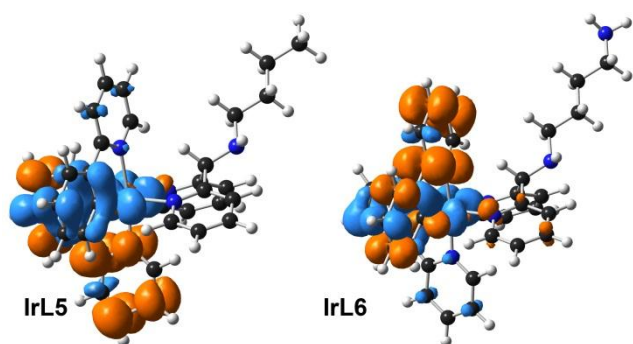


Figure 3. Electron density difference maps (EDDMs) of the lowest energy singlet–triplet electronic transition of **IrL5** and **IrL6** in their lowest-lying triplet state geometries. Blue indicates a decrease in charge density, while orange indicates an increase.

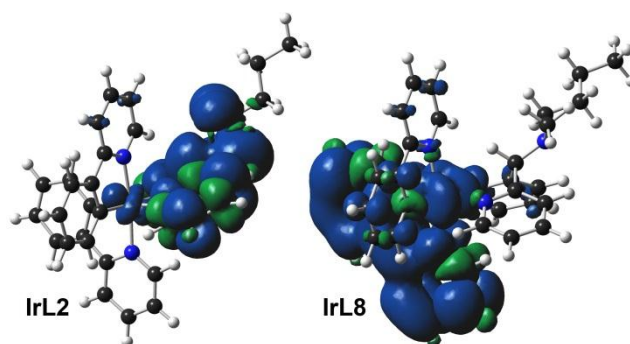


Figure 4. Contour plots of the spin density of the lowest-lying triplet-state geometry of complexes **IrL2** and **IrL8** (isovalue=0.004).

The spin density obtained for the lowest-lying triplet-state shows a triplet state centred over **L2**, involving the C=N bond (**Error! Reference source not found.**). This in agreement with the spectral shape and with the oxygen quenching of the emission observed experimentally.

Unfortunately, the Δ SCF and the TD-DFT approaches are unable to describe the emission process that takes place in the case of **IrL2**; both methods predict negative emission energy. The same situation was observed for the analogous complex $[\text{Ir}(\text{2-phenylpyridine})_2(\text{2,2'-(hydrazonomethylene)dipyridine})]^+$,²¹ suggesting that the weak emission occurs from orbitals at higher energies, quenched by the presence of π^* orbital located at lower energy. It is worth to note that triplet state optimized geometries (T_1) of the luminescent and non-luminescent Ir complexes show differences in the sequence of MO energies (Fig. ESI6). For the luminescent Ir complexes, *i.e.* $[\text{Ir}(\text{ppy})_2(\text{dipyridin-2-ylmethanol})]$,²¹ $[\text{Ir}(\text{ppy})_2(\text{3-hydroxy-3,3-di(pyridine-2-yl)propanenitrile})]$,²¹ **IrL5**, **IrL6** and **IrL8**, the HOMO and LUMO energies of the singlet states at T_1 geometries are very similar to the those of the singlet states at S_0 geometries. This roughly means that S_0 and T_1 geometries do not differ too much from each other and fast intersystem crossing is expected. The concept is analogue to the kinetic of the electron transfer introduced by Marcus⁵⁵ and adopted in electrochemistry where, whenever a reduction (or oxidation) follows a significant molecular reorganization, a slow heterogeneous electron transfer is expected.⁵⁶ For the non- or low-luminescent complexes, *i.e.* **IrL1**, $[\text{Ir}(\text{ppy})_2(\text{2,2'-(hydrazonomethylene)dipyridine})]$ ²¹ and **IrL2**, the HOMO and LUMO energies of the singlet states at T_1 and those at S_0 geometries significantly differ. In particular, HOMO and LUMO energies of the singlet states at T_1 are significantly less and more stable than those at S_0 geometries, respectively (*i.e.* the HOMO-LUMO gap is greatly decreased). Moreover, SOMO energies of the triplet state at T_1 geometries are particularly stabilized (especially if compared with LUMOs), so that their energies fall below those of the HOMO of the singlet states at the same T_1 geometry. This reflects the larger geometrical changes passing from S_0 to T_1 molecular structures, and we can forecast, if existing, a much slower intersystem crossing process from S_0 to T_1 . These considerations explain the wrong DFT prediction for the **IrL1** emission (C=O bond), as well as the negative emission energies predicted for those complexes with C=N bond. The experimentally observed low emissions are due to kinetic reasons, and originate from excited states at geometries different than the lowest-lying triplet states T_1 . In fact, the emission profile of these low-luminescent complexes (a part from low quantum yields and lifetimes difficult to measure) is very similar to the other strong-luminescent Ir complexes, suggesting that the emission occurs from excited states that are similar in shape and energies. This also tentatively explains one of the possible quenching mechanism (*via* molecular reorganization) followed by metal complexes containing functional groups that are electrochemically relatively easily reducible.

Electrochemistry

The electrochemical properties of complexes **IrL2**, **IrL5**, **IrL6-Boc**, **IrL6-TFA** and **IrL8** were studied by Cyclic Voltammetry (CV) in acetonitrile solutions (**Error! Reference source not found.**). The electrochemical behaviour of cationic iridium cyclometalated complexes is known (see our previous papers^{20,21} and references therein): 1e ligand-based reduction and 1e metal-based oxidation are generally observed, according to the nature of HOMO and LUMO. However, the presence of electro-reducible or electro-oxidizable moieties can significantly alter the electrochemical behaviour. The reversible and irreversible reduction processes at -1.59 and -1.78 V of **IrL2** very probably can be localized on the C=N functional group, whereas the irreversible oxidations observed for **IrL5** and **IrL8** almost certainly originate from the oxidation of amine groups.

Table 3. Electrochemically reversible half wave potentials ($E_{1/2}$) and chemically irreversible peak potentials (E_p) obtained from CV of **IrL** complexes at 0.2 V/s, GC electrode, in acetonitrile solutions (TBAPF₆ 0.1M). Potentials are vs. Fc(0/+1), used as internal standard.

Complex	Oxidations (V)	Reductions (V)
IrL2	$E_{1/2}=0.90, E_p=1.62$	$E_{1/2}=-1.59, E_p=-1.78, -2.13$
IrL5	$E_p=0.81, 0.93, 1.02, 1.66$	$E_p=-2.38, -2.62$
IrL6-Boc	$E_{1/2}=0.96, 1.29$	$E_p=-2.28, -2.55$
IrL6-TFA	$E_{1/2}=0.98, 1.15$	$E_p=-2.40, -2.68$
IrL8	$E_p=1.15, 1.55$	$E_p=-2.35, -2.66$

Anodic scan of **IrL5** shows several metal- and amine-centred irreversible oxidations, in the case of **IrL8** these processes probably overlap, whereas for **IrL6-Boc** and **IrL6-TFA** the protection of amine groups anodically shifts these oxidations. All iridium complexes, upon cathodic scan, show 1e electrochemically irreversible reductions between -2.13 and -2.40 V. These processes can be localized on the organic part of the **IrL** derivatives (see MO analysis and LUMO discussion in the computed geometries and electronic structures section).

Conclusions

The chemical reactivity and the spectroscopic, electrochemical and electronic properties of several heteroleptic iridium biscyclometalated complexes formally derived from 2,2'-dipyridylketone (**L1**) coordinated to the Ir metal has been investigated. We prove that the free and coordinated ligands have different reactivity towards amines, which in this case makes the synthesis of metal complexes feasible only starting from the preformed organic ligands. Although we forecast that the synthesis of Ir cyclometalated complexes containing a pendant amino group is feasible, diverse synthetic strategies should be employed, due to either **IrL1** reactivity or deprotection conditions of functional groups like Boc or TFA.

DFT calculated HOMO and LUMO shape and energies helped in the rationalization of the electrochemical behaviour of the Ir complexes under study. TD-DFT and Δ SCF calculations were carefully employed for the assignment of UV-vis absorptions and luminescent emissions.

In the interpretation of quantum mechanical calculations of excited states we also evidenced that care should be taken whenever remarkable geometrical differences are observed between singlet and triplet excited states. In these cases the lowest-lying triplet states (T_1) are significantly stabilized so that they cannot be the emitting state, and the observed luminescence (if any) should be due to excited states at higher energies with different geometries. The process of the molecular reorganization necessary to reach the T_1 geometry (at considerable lower energy) is then the responsible for both the quenching mechanism and the experimentally observed luminescence *via* kinetic considerations of the involved processes. Therefore the experimentally observed emission does not occur from the lowest-lying triplet state; at the same time the lowest-lying triplet state provides a possible non-radiative way to return to the ground state.

Experimental

Materials and methods

Di-2-pyridylketone (**L1**), 2-phenylpyridine, iridium trichloride, and all other reagents and solvents were of reagent grade and used as received without any further purification. Precursor dimer $[\text{Ir}(\text{ppy})_2(\mu\text{-Cl})]_2$,⁵⁷ and **IrL1**²⁰ were synthesized as previously reported. Acetonitrile was distilled over calcium hydride just before use. All the reactions involving the metal complexes or precursor were routinely performed under nitrogen atmosphere by using standard Schlenk techniques.

Electrochemistry was performed by a PC-controlled Autolab PGSTAT302N electrochemical analyser in the usual conditions,⁵⁸ using a standard three electrode cell configuration (glassy carbon working electrode, Pt counter electrode, aqueous 3 M KCl Calomel reference electrode). All measurements were carried out under Ar atmosphere, in acetonitrile solution with tetrabutylammonium hexafluorophosphate (TBAPF₆) 0.1 M as

supporting electrolyte, obtained as previously reported.⁵⁹ Positive feedback iR compensation was applied routinely and ferrocene (Fc) was used as an internal standard (half-wave potentials are reported against the Fc(0/+1) redox couple).

NMR spectra were recorded on a JEOL EX 400 spectrometer ($B_0 = 9.4$ T, ^1H operating frequency 399.78 MHz) with chemical shifts referenced to residual protons in the solvent. The following abbreviations are used: s, singlet; d, doublet; t, triplet; m, multiplet.

UV–Vis absorption spectra were measured with a double-beam Perkin–Elmer Lambda 20 UV–Vis spectrophotometer equipped with a 1 cm quartz cell. Room temperature emission spectra as well as luminescence lifetimes were obtained using a HORIBA Jobin Yvon IBH Fluorolog–TCSPC spectrofluorimeter. Fluorescence quantum yields Φ were determined by the comparative method, as previously reported.²¹ Luminescence lifetimes were determined by time-correlated single-photon counting. Excitation with nanosecond pulses of 297 nm light (repetition rate of 100 kHz) generated by a NanoLED pulsed diode was used. The emission data were collected using a spectral bandwidth of 2–10 nm. The data were collected into 2048 channels to 10,000 counts in the peak channel. The sample was maintained at 20 °C in an automated sample chamber (F-3004 Peltier Sample Cooler from Horiba Jobin Yvon IBH) for ambient temperature measurements. Emission decay data were analysed using the software DAS6 (TCSPC Decay Analysis Software).

Mass spectra were recorded using an XCT PLUS electrospray ionisation-ion trap (ESI–IT) mass spectrometer (Agilent Italy, Milan). In the spectra description the abbreviation [M] was used for the molecular ion. The reported values are in atomic mass units. Samples were dissolved in methanol. Scan range was 50–2000 m/z .

Computational details

Calculations were performed with the Gaussian 09 program package.⁶⁰ Geometry optimizations were performed in the gas phase, employing the DFT method for the ground state and the unrestricted Kohn–Sham formalism (UKS) for the lowest-lying triplet states. The nature of all stationary of the optimized geometries at singlet and triplet states was confirmed by normal-mode analysis, and no imaginary frequencies were found. The conductor-like polarizable continuum model (CPCM)^{61–63} with acetonitrile as the solvent was used to calculate the electronic structure and the excited states in solution. A total of 64 singlet and 8 triplet excited states were determined with a TD-DFT^{64,65} calculation, employing ground state geometries optimized in the gas phase. The emission energy was evaluated by the ΔSCF ⁶⁶ and TD-DFT^{67,68} approaches, taking into account the solvent effect with the CPCM method. The ΔSCF approach calculates the vertical energy gap between the ground state and the lowest-lying triplet state, both evaluated at the geometry optimized for lowest-lying triplet state and both computed using unrestricted wave functions (UKS). The TD-DFT approach calculates 8 triplet excited states as electronic transitions from the ground state, evaluated with lowest-lying triplet state geometry. This TD-DFT calculation uses a restricted wave function. GaussSum 2.2.4⁶⁹ was used to simulate the electronic spectra and to visualize the excited state transitions as electron density difference maps (EDDMs).^{70,71} All calculations employed the Becke three-parameter hybrid functional,⁷² and Lee Yang Parr’s gradient-corrected correlation functional (B3LYP).⁷³ The LanL2DZ basis set⁷⁴ and effective core potential were used for the Ir atom, and the 6-31G** basis set⁷⁵ was used for all other atoms.

Syntheses

N-(dipyridin-2-ylmethylene)butan-1-amine (L2). Five drops of acetic acid were added to a solution of di-2-pyridylketone (210 mg, 1.14 mmol) in 10 ml of methanol and butyl amine (292 mg, 4 mmol). After refluxing for 2 h, the solution was evaporated, the product, a yellow oil, washed with diethyl ether three times and dried. The product was obtained in high yields after column chromatography on silica gel, using CH_2Cl_2 – CH_3OH (98 : 2) as eluent.

^1H NMR ([D6]acetone, 400 MHz) δ : 8.65 (d, $J=4.83$ Hz, 1H), 8.39 (d, $J=4.83$, 1H), 8.26 (d, $J=8.49$ Hz, 1H), 7.86 (t, $J=7.69$, 2H), 7.36 (t, $J=11.57$, 2H), 7.30 (d, $J=8.35$), 3.39 (t, $J=7.03$, 2H), 1.65 (q, $J=7.35$ Hz, 2H),

1.37 (m, $J=7.45$, 2H), 0.87 (t, $J=7.57$, 3H). ^{13}C NMR ([D6]acetone, 100 MHz) δ : 167.28, 158.37, 156.66, 150.08, 149.10, 136.90, 136.29, 124.95, 124.46, 123.74, 122.26, 56.77, 33.86, 21.19, 14.15. MS (ESI⁺): $m/z = 240.45$ [M+H]⁺.

N1-(dipyridin-2-ylmethylene)butane-1,4-diamine (L3). Di-2-pyridyl ketone (300 mg, 1.63 mmol), butane-1,4-diamine (putrescine) (1 mL, 9.01 mmol) and 5 drops of glacial acetic acid were mixed in 30 ml of methanol. After refluxing 2 h, the solution was cooled, solvent evaporated and the oil product dried under vacuum. The product was obtained in high yields after column chromatography on silica gel, using CH₂Cl₂–CH₃OH (98 : 2) as eluent.

^1H NMR ([D6]acetone, 400 MHz) δ : 8.63 (d, $J=7.5$ Hz, 1H), 8.39 (d, $J=7.3$ Hz, 1H), 8.25 (t, $J=8.05$ Hz, 1H), 7.88-7.82 (m, 2H), 7.39-7.27 (m, 3H), 3.43-3.37 (m, 2H), 3.19-3.13 (2H), 1.78-1.71 (m, 3H), 1.66-1.59 (m, 2H). ^{13}C NMR ([D6]acetone, 100 MHz) δ : 167.4, 158.2, 156.7, 150.1, 149.1, 137.1, 136.3, 125.0, 124.7, 123.7, 122.3, 54.0, 53.0, 51.7, 51.0. MS (ESI⁺): $m/z = 255.33$ [M+H]⁺.

N1,N4-bis(dipyridin-2-ylmethylene)butane-1,4-diamine (L4). Five drops of acetic acid, di-2-pyridyl ketone (839 mg, 4.56 mmol) and butane-1,4-diamine (putrescine) (200 mg, 2.28 mmol, 2 mmol) were refluxed in 10 mL of methanol for 4 h. The solution was cooled and the solvent removed under vacuum. The product was obtained in high yields after column chromatography on silica gel, using CH₂Cl₂–CH₃OH (98 : 2) as eluent.

^1H NMR ([D6]acetone, 400 MHz) δ : 8.47 (d, $J=4.83$ Hz, 4H), 7.67 (t, $J=7.76$, 4H), 7.46 (d, $J=8.05$ Hz, 4H), 7.17 (t, $J=6.15$, 4H), 5.02 (s, 2H), 2.57-2.54 (m, 4H), 2.08-2.06 (m, 2H), 1.57 (ses, $J=3.25$ Hz, 4H), 0.86 (t, $J=7.35$, 3H). ^{13}C NMR ([D6]acetone, 100 MHz) δ : 167.43, 158.12, 156.68, 149.99, 149.10, 137.15, 136.51, 124.94, 124.63, 123.68, 122.33, 53.78, 28.80. MS (ESI⁺): $m/z = 443.4$ [M+H]⁺.

N-(dipyridin-2-ylmethyl)butan-1-amine (L5). **L2** (500 mg, 2.09 mmol) and an excess of NaBH₄ (350 mg, 5 mmol) were added to methanol (30 ml) and kept at 0°C for 1 h. After evaporation of solvent the compound was dissolved in CH₂Cl₂, and the solution washed with water and brine, filtered and evaporated. The solid washed three times with diethyl ether and dried (479 mg, 1.99 mmol, 95% yield).

^1H NMR ([D6]acetone, 400 MHz) δ : 8.48 (d, $J=4.83$ Hz, 2H), 7.69 (t, $J=7.69$, 2H), 7.46 (d, $J=7.90$ Hz, 2H), 7.19 (t, $J=6.22$, 2H), 5.00 (s, 1H), 2.54 (t, $J=6.69$), 1.49 (q, $J=7.21$, 2H), 1.35 (m, $J=9.26$ Hz, 2H), 0.86 (t, $J=7.35$, 3H). ^{13}C NMR ([D6]acetone, 100 MHz) δ : 163.39, 149.46, 137.01, 122.95, 122.75, 70.17, 48.38, 33.15, 21.03, 14.31. MS (ESI⁺): $m/z = 242.3$ [M+H]⁺.

N1-(dipyridin-2-ylmethyl)butane-1,4-diamine. (L6). **L3** was treated with an excess of NaBH₄ in methanol at 0°C for 1h. After evaporation of solvent the compound was dissolved in CH₂Cl₂, the solution washed with water and brine, filtered, dried over Na₂SO₄ and evaporated. The oil product was obtained in high yields after washing three times with petroleum ether and drying.

^1H NMR ([D6]acetone, 400 MHz) δ : 8.48 (d, $J=5.7$ Hz, 2H), 7.70 (t, $J=8.3$ Hz, 2H), 7.47 (d, $J=8.20$ Hz, 2H), 7.18 (t, $J=5.6$ Hz, 2H), 5.00 (s, 1H), 3.14 (t, $J=7.05$ Hz, 2H), 2.60-2.54 (t, 2H), 1.63-1.51 (m, 4H). ^{13}C NMR ([D6]acetone, 100 MHz) δ : 162.5, 148.8, 136.4, 122.2, 122.0, 69.4, 50.9, 47.6, 28.6, 28.1. MS (ESI⁺): $m/z = 257.35$ [M+H]⁺.

L6-Boc. *N-tert*-Butyloxycarbonylation (Boc) of **L6** was carried out by stirring a mixture of **L6** (441 mg, 1.72 mmol) and (Boc)₂O (826 mg, 3.78 mmol) in water (3 mL) at room temperature (25-30 °C). Transparent liquid droplets were formed and a white emulsion appeared on the walls of the reaction vessel with slow effervescence. After 1 h a white solid precipitated. The reaction was treated with EtOAc (5 mL), the EtOAc layer was separated and the aqueous part extracted with EtOAc (2×5 ml). The combined EtOAc extracts were washed with water (2×3 mL), dried (Na₂SO₄) and evaporated to give a yellow oily residue, which was purified by column chromatography (eluent CH₂Cl₂–CH₃OH 98 : 2) to give 458 mg, 1.28 mmol, 74.4% yield. ^1H NMR ([D1]chloroform, 400 MHz) δ : 8.58 (d, $J=5.10$ Hz, 2H), 7.67 (t, $J=8.00$ Hz, 2H), 7.29 (d, $J=7.86$ Hz, 2H), 7.19 (t, $J=5.90$ Hz, 2H), 6.44 (s, 1H), 3.40 (t, $J=7.60$ Hz, 2H), 2.94-2.89 (m, 2H), 1.39-1.34 (m, 11H), 1.26-1.22 (m, 2H). ^{13}C NMR ([D1]chloroform, 100 MHz) δ : 159.51, 156.16, 149.50, 136.90, 126.50, 122.41, 80.31, 79.29, 45.92, 40.33, 40.07, 28.63, 27.56, 27.16. MS (ESI⁺): $m/z = 456.81$ [M+H]⁺.

L6-Fmoc. Crude **L6** (350 mg, 1.37 mmol) and potassium carbonate (200 mg, 1.45 mmol) were suspended in

water-acetonitrile mixture (50:50, 20 mL) and stirred at room temperature for 10 minutes. N-(9-fluorenylmethoxycarbonyl) (Fmoc) succinimide (800 mg, 2.37 mmol) dissolved in acetonitrile (8 mL) was slowly added and stirred for 10 h. The solution was extracted with CH₂Cl₂ (5×5 mL), the CH₂Cl₂ layer separated and the aqueous part extracted with CH₂Cl₂ (2×5mL). The combined CH₂Cl₂ extracts were washed with water (2×3mL), dried over Na₂SO₄ and evaporated to give a yellow oily residue, which was purified by column chromatography on Al₂O₃ (eluent CH₂Cl₂-CH₃OH 99-1) to give 202 mg, 0.289 mmol, 21.1% yield.

¹H NMR ([D1]chloroform, 400 MHz) δ: 8.60 (d, *J*=4.80 Hz, 2H), 7.76-7.68 (m, 6H), 7.65-7.50 (m, 5H), 7.40-7.37 (m, 4H), 7.32-7.29 (m, 11H), 5.55 (s, 1H), 4.34 (d, *J*=7.180 Hz, 4H), 4.20 (d, *J*=7.18 Hz, 2H), 3.25-3.18 (m, 2H), 3.05-3.01 (m, 2H), 2.03-1.97 (m, 2H), 1.65-1.60 (m, 2H). ¹³C NMR ([D1]chloroform, 100 MHz) δ: 158.9, 156.0, 155.1, 148.6, 138.8, 137.2, 136.2, 135.2, 133.0, 132.8, 131.5, 126.4, 125.7, 125.0, 124.1, 120.6, 118.0, 60.5, 58.8, 50.3, 45.2, 35.8, 27.2.

L6-TFA. To a solution of **L6** (364 mg, 1.42 mmol) in dry THF (10 mL) was slowly added ethyl trifluoroacetate (0.372 mL, 3.13 mmol) at 0°C. After stirring for 10 h at room temperature the mixture was concentrated in vacuum, diluted with EtOAc-H₂O (50:50, 8 mL). The EtOAc layer was separated and the aqueous part extracted with EtOAc (2×3 mL). The combined EtOAc extracts were washed with water (2×3 mL), dried over Na₂SO₄ and evaporated to give a yellow oily residue (200 mg, 0.568 mmol, 40.0% yield).

¹H NMR ([D1]chloroform, 400 MHz) δ: 8.61 (d, *J*=6.78 Hz, 2H), 7.73 (t, *J*=7.86 Hz, 2H), 7.40 (d, *J*=7.90 Hz, 2H), 7.30 (t, *J*=6.15 Hz, 2H), 5.66 (s, 1H), 3.37 (m, 2H), 3.09 (t, *J*=7.35Hz, 2H), 1.92 (m, 2H), 1.71 (m, 2H). ¹³C NMR ([D1]chloroform, 100 MHz) δ: 153.14, 150.10, 138.00, 124.3, 123.3, 65.08, 45.5, 38.6, 25.20, 23.56. MS (ESI⁺): *m/z* = 448.37 [M+H]⁺, 352.35 [M-TFA]⁺.

N1,N4-bis(dipyridin-2-ylmethyl)butane-1,4-diamine (L7). A solution of **L4** in methanol containing an excess of NaBH₄ at 0 °C was stirred for 1 h. After solvent evaporation the ligand was dissolved in CH₂Cl₂, the solution filtered and the solvent removed under vacuum. The solid was washed with diethyl ether three times. The product was obtained in high yields after column chromatography on silica gel, using CH₂Cl₂-CH₃OH (98 : 2) as eluent.

¹H NMR ([D6]acetone, 400 MHz) δ: 8.63 (d, *J*=4.98 Hz, 2H), 8.39 (d, *J*=4.39, 2H), 8.24 (d, *J*=8.05 Hz, 2H), 7.87-7.81 (m, 4H), 7.37-7.32 (m, 4H), 7.27 (d, *J*=7.76, 2H), 3.42-3.38 (m, 4H), 1.76(q, *J*=2.96, 4H). ¹³C NMR ([D6]acetone, 100 MHz) δ: 163.36, 149.62, 137.11, 122.99, 122.77, 70.34, 48.53, 28.80. MS (ESI⁺): *m/z* = 425.4 [M+H]⁺.

N-(dipyridin-2-ylmethyl)-N-methylbutan-1-amine (L8). 93 mg of **L5** (0.386 mmol) was treated with a solution of CH₃I (0.119 mL, 1.93 mmol) in dry CHCl₃ (5 mL) for 2.5 h at room temperature. Water (8 mL) was added and the solution extracted with CH₂Cl₂ (3×2 mL). Evaporation of the solvent gave a crude product (62 mg, 0.243 mmol, 62.3 %).

¹H NMR ([D1]chloroform, 400 MHz) δ: 8.65 (d, *J*=5.70 Hz, 2H), 7.89 (d, *J*=7.61 Hz, 2H), 7.78 (t, *J*=7.76 Hz, 2H), 7.32 (t, *J*=6.30 Hz, 2H), 6.55 (s, 1H), 3.34 (t, *J*=8.05 Hz, 2H), 2.99 (s, 3H), 1.88-1.79 (m, 2H), 1.37-1.30 (m, 2H), 0.89 (t, *J*=7.32 Hz, 2H). ¹³C NMR ([D1]chloroform, 100 MHz) δ: 149.91, 138.19, 125.16, 124.50, 55.48, 49.78, 39.89, 26.28, 19.74, 13.62.

[Ir(ppy)₂(N-(dipyridin-2-ylmethylene)butan-1-amine)]Cl ([Ir-L2]Cl). [Ir(ppy)₂(μ-Cl)]₂ dimer and **L2** (molar ratio of 1:2.1) were stirred at reflux in a 50:50 mixture of CH₃OH and CH₂Cl₂ for 1 h. The solvent was removed in vacuum and the complexes purified by column chromatography on silica (CH₂Cl₂:CH₃OH 98:2).

¹H NMR ([D6]acetone, 400 MHz) δ: 8.90 (s, 1H), 8.48 (s, 1H), 8.32 (d, *J*=8.10 Hz, 1H), 8.25 (d, *J*=8.40, 1H), 8.19-8.05 (m, 4H), 8.04-8.00 (m, 2H), 7.88 (d, *J*=8.05 Hz, 2H), 7.76-7.70 (m, 2H), 7.59 (d, *J*=6.88, 1H), 7.42 (t, *J*=6.52 Hz, 1H), 7.33 (t, *J*=6.81 Hz, 1H), 7.03 (t, *J*=7.54, 1H), 6.98 (t, *J*=7.47 Hz, 1H), 6.92 (t, *J*=7.47, 1H), 6.86 (t, *J*=7.47 Hz, 1H), 6.39 (d, *J*=7.76, 1H), 6.24 (d, *J*=7.76 Hz, 1H), 3.65-3.52 (m, 2H), 0.61 (m, *J*=7.47 Hz, 2H), 0.32 (t, *J*=7.32 Hz, 3H). ¹³C NMR ([D6]acetone, 100 MHz) δ: 176.16, 168.97, 157.40, 151.84, 150.95, 144.97, 140.29, 139.77, 139.72, 138.65, 132.76, 131.93, 131.47, 131.35, 130.88, 130.80, 126.57, 125.79, 125.68, 125.49, 124.72, 123.61, 120.86, 57.90, 31.77, 20.64, 13.27. MS (ESI⁺): *m/z* = 740.1 [M]⁺.

IrL3. Reaction of $\text{Ir}(\text{ppy})_2(\mu\text{-Cl})_2$ dimer with **L3** gave a large variety of products, with very low yields and difficult to separate.

IrL4. Reaction of **L4** with $\text{Ir}(\text{ppy})_2(\mu\text{-Cl})_2$ in condition similar to those used for **IrL2** gave several products. From the reaction mixture **IrL1** was separated and characterized.

$[\text{Ir}(\text{ppy})_2(N\text{-}(\text{dipyridin-2-ylmethyl})\text{butan-1-amine})]\text{Cl}$ (IrL5Cl**).** The reaction was carried out as for **IrL2** (yield 60%).

^1H NMR ([D6]acetone, 400 MHz) δ : 8.98 (d, $J=5.86$ Hz, 1H), 8.48 (d, $J=4.69$ Hz, 1H), 8.24 (d, $J=7.91$ Hz, 1H), 8.09 (t, $J=7.91$ Hz, 2H), 8.01-7.95 (m, 3H), 7.90-7.87 (m, 2H), 7.80-7.71 (m, 3H), 7.44 (t, $J=6.45$ Hz, 2H), 7.37 (t, $J=6.70$, 1H), 7.24 (t, $J=6.60$ Hz, 1H), 7.02 (d, $J=8.10$ Hz, 1H), 6.97 (t, $J=7.75$, 1H), 6.92 (t, $J=7.47$ Hz, 1H), 6.84 (t, $J=7.32$ Hz, 1H), 6.78 (t, $J=7.47$, 1H), 6.28 (d, $J=7.61$ Hz, 1H), 6.21 (d, $J=7.61$ Hz, 1H), 6.10 (d, $J=10.00$ Hz, 1H), 6.10 (d, $J=10.00$ Hz, 1H), 6.10 (d, $J=10.00$ Hz, 1H), 6.10 (d, $J=10.00$ Hz, 1H). ^{13}C NMR ([D6]acetone, 100 MHz) δ : 170.54, 169.85, 164.67, 158.55, 152.38, 151.96, 150.57, 145.57, 145.18, 140.30, 139.73, 139.60, 139.18, 133.02, 132.46, 131.58, 131.44, 126.74, 126.67, 126.62, 125.86, 125.80, 125.69, 124.69, 124.58, 123.40, 123.16, 121.04, 120.92, 74.08, 53.99, 31.71, 20.17, 13.40. MS (ESI⁺): $m/z = 741.3$ [M]⁺.

IrL6-Boc. $[\text{Ir}(\text{ppy})_2\text{Cl}]_2$ (150 mg, 0.138 mmol) and **L6-Boc** (548 mg, 1.54 mmol) reacted in $\text{CH}_3\text{OH}:\text{CH}_2\text{Cl}_2$ mixture (50:50, 20 mL) for 1 h at reflux. The crude product was purified by column chromatography on silica ($\text{CH}_2\text{Cl}_2:\text{CH}_3\text{OH}$ 96:4) to give 162 mg (0.189 mmol, 68.47% yield) of **IrL6-Boc**.

^1H NMR ([D1]chloroform, 400 MHz) δ : 8.50 (s, 2H), 8.30 (s, 2H), 8.14 (d, $J=9.23$ Hz, 2H), 7.96-7.83 (m, 3H), 7.79 (d, $J=9.23$ Hz, 2H), 7.72-7.59 (m, 2H), 7.54 (d, $J=8.20$ Hz, 1H), 7.45 (d, $J=9.23$ Hz, 2H), 7.18-7.12 (m, 2H), 7.00 (t, $J=7.18$ Hz, 2H), 6.91 (t, $J=6.66$ Hz, 2H), 6.79 (t, $J=7.52$ Hz, 2H), 6.20 (d, $J=7.18$ Hz, 1H), 6.10 (d, $J=7.18$ Hz, 1H), 5.75 (s, 1H), 4.90-4.78 (m, 2H), 3.08-3.01 (m, 2H), 1.42-1.36 (m, 13H). ^{13}C NMR ([D1]chloroform, 100 MHz) δ : 168.89, 167.59, 156.17, 152.17, 149.48, 143.16, 139.22, 139.11, 132.07, 131.09, 130.99, 130.46, 125.62, 125.50, 125.17, 124.52, 123.61, 123.09, 122.77, 120.55, 120.42, 82.81, 78.89, 53.50, 39.98, 28.43, 27.65. MS (ESI⁺): $m/z = 956.80$ [M]⁺, 856.83 [M-Boc]⁺.

Attempts to synthesise **IrL6-Fmoc** failed, giving several decomposition products.

Ir-L6-TFA. $[\text{Ir}(\text{ppy})_2\text{Cl}]_2$ (275 mg, 0.254 mmol) and **L6-TFA** (190 mg, 0.5398 mmol) reacted in $\text{CH}_3\text{OH}:\text{CH}_2\text{Cl}_2$ mixture (50:50, 20 mL) for 1h at reflux. The crude product was purified by column chromatography on Al_2O_3 two times ($\text{CH}_2\text{Cl}_2:\text{CH}_3\text{OH}$ 99:1) to give 153 mg (0.179 mmol, 35.0% yield) of **Ir-L6-TFA**.

^1H NMR ([D1]chloroform, 400 MHz) δ : 9.56 (d, $J=5.47$ Hz, 1H), 8.79 (s, 1H), 8.49 (d, $J=7.52$ Hz, 1H), 8.28 (d, $J=5.44$ Hz, 1H), 7.95-7.92 (m, 2H), 7.84-7.78 (m, 3H), 7.61-7.56 (m, 2H), 7.37 (d, $J=7.52$ Hz, 1H), 7.25-7.19 (m, 2H), 7.04-6.78 (m, 8H), 6.29 (d, $J=7.52$ Hz, 1H), 6.20 (d, $J=7.52$ Hz, 1H), 4.73 (s, 1H), 3.02-2.84 (m, 4H), 1.97-1.84 (m, 4H). ^{13}C NMR ([D1]chloroform, 100 MHz) δ : 169.39, 167.18, 165.18, 159.30, 153.46, 152.01, 150.99, 150.01, 149.80, 149.30, 149.20, 148.90, 147.90, 144.21, 143.25, 140.13, 138.91, 138.58, 138.11, 137.95, 137.63, 132.54, 131.95, 131.45, 131.01, 130.87, 130.31, 130.11, 128.91, 126.01, 125.83, 125.08, 124.79, 124.45, 124.37, 124.04, 123.82, 123.43, 122.69, 122.14, 120.17, 119.72, 118.96, 71.12, 52.96, 38.19, 26.33, 24.80. MS (ESI⁺): $m/z = 951.00$ [M]⁺, 853.15 [M-TFA]⁺.

IrL7. Reaction of **L7** with $\text{Ir}(\text{ppy})_2(\mu\text{-Cl})_2$ in condition similar to those used for **IrL2** gave several products. From the reaction mixture **IrL1** was separated and characterized.

$[\text{Ir}(\text{ppy})_2(N\text{-}(\text{dipyridin-2-ylmethyl})\text{-}N\text{-methylbutan-1-amine})]\text{Cl}$ (IrL8Cl**).** A suspension of $[\text{Ir}(\text{ppy})_2\text{Cl}]_2$ (120 mg, 0.111 mmol) and **L8** (50 mg, 0.196 mmol) in $\text{CH}_2\text{Cl}_2:\text{CH}_3\text{OH}$ 1:1 mixture (20 mL) was heated to reflux and stirred under inert atmosphere for 2 h. The resulting brown solution was cooled to room temperature and the solution volume reduced to about 10 mL. The crude product was purified by column chromatography on Al_2O_3 (CH_2Cl_2) to give 27 mg (0.035 mmol, 17.8% yield).

^1H NMR ([D1]chloroform, 400 MHz) δ : 8.26 (d, $J=5.86$ Hz, 1H), 8.10 (d, $J=8.10$ Hz, 2H), 7.97-7.77 (m, 12H), 7.70 (d, $J=7.91$ Hz, 1H), 7.23 (t, $J=6.59$ Hz, 1H), 7.12-7.05 (m, 2H), 6.94-6.85 (m, 4H), 6.19 (d, $J=7.61$ Hz, 1H), 6.16 (d, $J=7.61$ Hz, 1H), 5.14 (s, 1H), 1.89-1.85 (m, 5H), 1.29-1.19 (m, 2H), 0.92-0.83 (m, 2H), 0.68 (t, $J=7.76$ Hz, 3H). ^{13}C NMR ([D1]chloroform, 100 MHz) δ : 168.41, 167.95, 159.52, 155.14, 154.15,

153.69, 149.92, 148.01, 145.96, 145.51, 140.38, 139.98, 139.54, 139.31, 133.06, 132.97, 131.09, 130.98, 129.89, 129.45, 127.27, 127.19, 126.68, 126.20, 125.29, 124.45, 124.16, 123.86, 123.61, 122.11, 121.24, 119.25, 77.23, 53.58, 39.84, 26.20, 21.05, 14.02. MS (ESI⁺): m/z = 756.16 [M]⁺.

Acknowledgements

C.G. thanks Regione Piemonte for financial support.

References

- 1 L. Flamigni, A. Barbieri, C. Sabatini, B. Ventura, and F. Barigelletti. Photochemistry and Photophysics of Coordination Compounds: Iridium. 143-203. 2007. Berlin, Springer-Verlag. Topics in current chemistry.
- 2 P. T. Chou and Y. Chi, *Chem. Eur. J.*, 2007, **13**, 380-395.
- 3 H. A. Al-Attar, G. C. Griffiths, T. N. Moore, M. Tavasli, M. A. Fox, M. R. Bryce, and A. P. Monkman, *Adv. Funct. Mater.*, 2011, **21**, 2376-2382.
- 4 Y. T. Tao, C. L. Yang, and J. G. Qin, *Chem. Soc. Rev.*, 2011, **40**, 2943-2970.
- 5 D. L. Davies, M. P. Lowe, K. S. Ryder, K. Singh, and S. Singh, *Dalton Trans.*, 2011, **40**, 1028-1030.
- 6 V. N. Kozhevnikov, K. Dahms, and M. R. Bryce, *J. Org. Chem.*, 2011, **76**, 5143-5148.
- 7 C. Schaffner-Hamann, A. von Zelewsky, A. Barbieri, F. Barigelletti, G. Muller, J. P. Riehl, and A. Neels, *J. Am. Chem. Soc.*, 2004, **126**, 9339-9348.
- 8 M. D. Ward, *Chem. Soc. Rev.*, 1997, **26**, 365-375.
- 9 A. Ruggi, M. Berenguel Alonso, D. N. Reinhoudt, and A. H. Velders, *Chem. Commun.*, 2010, **46**, 6726-6728.
- 10 F. Schmitt, P. Govindaswamy, G. Suss-Fink, W. H. Ang, P. J. Dyson, L. Juillerat-Jeanneret, and B. Therrien, *J. Med. Chem.*, 2008, **51**, 1811-1816.
- 11 P. I. Djurovich, D. Murphy, M. E. Thompson, B. Hernandez, R. Gao, P. L. Hunt, and M. Selke, *Dalton Trans.*, 2007, 3763-3770.
- 12 R. M. Edkins, S. L. Bettington, A. E. Goeta, and A. Beeby, *Dalton Trans.*, 2011, doi:10.1039/C1DT11164G.
- 13 A. J. Morris, G. J. Meyer, and E. Fujita, *Acc. Chem. Res.*, 2009, **42**, 1983-1994.
- 14 B. Loges, A. Boddien, H. Junge, J. R. Noyes, W. Baumann, and M. Beller, *Chem. Commun.*, 2009, 4185-4187.
- 15 F. Gartner, B. Sundararaju, A. E. Surkus, A. Boddien, B. Loges, H. Junge, P. H. Dixneuf, and M. Beller, *Angew. Chem. Int. Ed.*, 2009, **48**, 9962-9965.
- 16 P. Zhang, M. Wang, Y. Na, X. Li, Y. Jiang, and L. Sun, *Dalton Trans.*, 2010, **39**, 1204-1206.
- 17 P. N. Curtin, L. L. Tinker, C. M. Burgess, E. D. Cline, and S. Bernhard, *Inorg. Chem.*, 2009, **48**, 10498-10506.
- 18 L. L. Tinker and S. Bernhard, *Inorg. Chem.*, 2009, **48**, 10507-10511.
- 19 D. Hanss, J. C. Freys, G. Bernardinelli, and O. S. Wenger, *Eur. J. Inorg. Chem.*, 2009, 4850-4859.
- 20 G. Volpi, C. Garino, L. Salassa, J. Fiedler, K. I. Hardcastle, R. Gobetto, and C. Nervi, *Chem. Eur. J.*, 2009, **15**, 6415-6427.
- 21 G. Volpi, C. Garino, E. Breuza, R. Gobetto, and C. Nervi, *J. Chem. Soc., Dalton Trans.*, 2012, **41**, 1065-1073.
- 22 J. Suh and D. W. Min, *J. Org. Chem.*, 1991, **56**, 5710-5712.
- 23 C. Hemmert, M. Renz, H. Gornitzka, and B. Meunier, *J. Chem. Soc., Dalton Trans.*, 1999, 3989-3994.
- 24 A. G. J. Ligtenbarg, A. L. Spek, R. Hage, and B. L. Feringa, *J. Chem. Soc., Dalton Trans.*, 1999, 659-661.
- 25 O. Adidou, C. Goux-Henry, M. Safi, M. Soufiaoui, and E. Framery, *Tetrahedron Lett.*, 2008, **49**, 7217-7219.
- 26 R. L. McCreery, *Chem. Rev.*, 2008, **108**, 2646-2687.
- 27 K. Balasubramanian and M. Burghard, *Small*, 2005, **1**, 180-192.
- 28 B. Barbier, J. Pinson, G. Desarmot, and M. Sanchez, *J. Electrochem. Soc.*, 1990, **137**, 1757-1764.
- 29 C. Combellas, M. Delamar, F. Kanoufi, J. Pinson, and F. I. Podvorica, *Chem. Mater.*, 2005, **17**, 3968-3975.
- 30 J. Pinson and F. Podvorica, *Chem. Soc. Rev.*, 2005, **34**, 429-439.
- 31 M. Sandroni, G. Volpi, J. Fiedler, R. Buscaino, G. Viscardi, L. Milone, R. Gobetto, and C. Nervi, *Catal. Today*, 2010, **158**, 22-28.

- 32 B. Flores-Chavez, B. A. Martinez-Ortega, J. G. varado-Rodriguez, and N. ndrade-Lopez, *J. Chem. Cryst.*, 2005, **35**, 451-456.
- 33 B. Karimi, A. Zamani, and J. H. Clark, *Organometallics*, 2005, **24**, 4695-4698.
- 34 V. Balzani, A. Juris, M. Venturi, S. Campagna, and S. Serroni, *Chem. Rev.*, 1996, **96**, 759-833.
- 35 A. Juris, V. Balzani, F. Barigelletti, S. Campagna, P. Belser, and A. Vonzelewsky, *Coord. Chem. Rev.*, 1988, **84**, 85-277.
- 36 K. D. Demadis, C. M. Hartshorn, and T. J. Meyer, *Chem. Rev.*, 2001, **101**, 2655-2685.
- 37 S. Welter, K. Brunner, J. W. Hofstraat, and L. De Cola, *Nature*, 2003, **421**, 54-57.
- 38 P. J. Low, *Dalton Trans.*, 2005, 2821-2824.
- 39 J. D. Ortego and J. Meynig, *J. Chem. Eng. Data*, 1986, **31**, 365-366.
- 40 C. J. Sumby and P. J. Steel, *New J. Chem.*, 2005, **29**, 1077-1081.
- 41 A. J. Canty and N. J. Minchin, *Aust. J. Chem.*, 1986, **39**, 1063-1069.
- 42 D. M. D'Alessandro, F. R. Keene, P. J. Steel, and C. J. Sumby, *Aust. J. Chem.*, 2003, **56**, 657-664.
- 43 K. Q. Ling, W. S. Li, and L. M. Sayre, *J. Am. Chem. Soc.*, 2008, **130**, 933-944.
- 44 M. E. Bluhm, M. Ciesielski, H. Gorls, and M. Doring, *Angew. Chem. Int. Ed.*, 2002, **41**, 2962-2965.
- 45 H. Ding and G. K. Friestad, *Org. Lett.*, 2004, **6**, 637-640.
- 46 M. Prashad, B. Hu, D. Har, O. Repic, and T. J. Blacklock, *Tetrahedron Lett.*, 2000, **41**, 9957-9961.
- 47 C. Spencer, J. Balsells, and H. M. Li, *Tetrahedron Lett.*, 2009, **50**, 1010-1012.
- 48 C. Visintin, A. E. Aliev, D. Riddall, D. Baker, M. Okuyama, P. M. Hoi, R. Hiley, and D. L. Selwood, *Org. Lett.*, 2005, **7**, 1699-1702.
- 49 S. V. Chankeshwara and A. K. Chakraborti, *Org. Lett.*, 2006, **8**, 3259-3262.
- 50 D. K. Mohapatra and K. A. Durugkar, *Arkivoc*, 2005, 20-28.
- 51 D. Q. Xu, K. Prasad, O. Repic, and T. J. Blacklock, *Tetrahedron Lett.*, 1995, **36**, 7357-7360.
- 52 S. Zalis, C. Consani, A. El Nahhas, A. Cannizzo, M. Chergui, F. Hartl, and A. Vlcek, *Inorg. Chim. Acta*, 2011, **374**, 578-585.
- 53 C. Dragonetti, L. Falcicola, P. Mussini, S. Righetto, D. Roberto, R. Ugo, A. Valore, F. De Angelis, S. Fantacci, A. Sgamellotti, M. Ramon, and M. Muccini, *Inorg. Chem.*, 2007, **46**, 8533-8547.
- 54 Y. You and S. Y. Park, *Dalton Trans.*, 2009, 1267-1282.
- 55 R. A. Marcus, *J. Chem. Phys.*, 1957, **26**, 867-871.
- 56 P. Zanello, C. Nervi, and F. Fabrizi De Biani, *Inorganic Electrochemistry. Theory, Practice and Application*, RSC, Cambridge, 2011.
- 57 S. Sprouse, K. A. King, P. J. Spellane, and R. J. Watts, *J. Am. Chem. Soc.*, 1984, **106**, 6647-6653.
- 58 E. Rosenberg, M. J. Abedin, D. Rokhsana, D. Osella, L. Milone, C. Nervi, and J. Fiedler, *Inorg. Chim. Acta*, 2000, **300**, 769-777.
- 59 A. Albertino, C. Garino, S. Ghiani, R. Gobetto, C. Nervi, L. Salassa, E. Rosenberg, A. Sharmin, G. Viscardi, R. Buscaino, G. Croce, and M. Milanese, *J. Organomet. Chem.*, 2007, **692**, 1377-1391.
- 60 M. J. Frisch, G. W. Trucks, H. B. Schlegel, G. E. Scuseria, M. A. Robb, J. R. Cheeseman, G. Scalmani, V. Barone, B. Mennucci, G. A. Petersson, H. Nakatsuji, M. Caricato, X. Li, H. P. Hratchian, A. F. Izmaylov, J. Bloino, G. Zheng, J. L. Sonnenberg, M. Hada, M. Ehara, K. Toyota, R. Fukuda, J. Hasegawa, M. Ishida, T. Nakajima, Y. Honda, O. Kitao, H. Nakai, T. Vreven, J. A. Jr. Montgomery, J. R. Peralta, F. Ogliaro, M. Bearpark, J. J. Heyd, E. Brothers, K. N. Kudin, V. N. Staroverov, R. Kobayashi, J. Normand, K. Raghavachari, A. Rendell, J. C. Burant, S. S. Iyengar, J. Tomasi, M. Cossi, N. Rega, J. Millam, M. Klene, J. E. Knox, J. B. Cross, V. Bakken, C. Adamo, J. Jaramillo, R. Gomperts, R. E. Stratmann, O. Yazyev, A. J. Austin, R. Cammi, C. Pomelli, J. Ochterski, R. L. Martin, K. Morokuma, V. G. Zakrzewski, G. A. Voth, P. Salvador, J. J. Dannenberg, S. Dapprich, A. D. Daniels, O. Farkas, J. B. Foresman, J. V. Ortiz, J. Cioslowski, and D. J. Fox. Gaussian 09. [Revision A.02]. 2009. Wallingford CT, Gaussian, Inc.
- 61 V. Barone and M. Cossi, *J. Phys. Chem. A*, 1998, **102**, 1995-2001.
- 62 M. Cossi and V. Barone, *J. Chem. Phys.*, 2001, **115**, 4708-4717.
- 63 M. Cossi, N. Rega, G. Scalmani, and V. Barone, *J. Comput. Chem.*, 2003, **24**, 669-681.
- 64 M. E. Casida, C. Jamorski, K. C. Casida, and D. R. Salahub, *J. Chem. Phys.*, 1998, **108**, 4439-4449.
- 65 R. E. Stratmann, G. E. Scuseria, and M. J. Frisch, *J. Chem. Phys.*, 1998, **109**, 8218-8224.
- 66 A. Vlcek and S. Zališ, *Coord. Chem. Rev.*, 2007, **251**, 258-287.
- 67 S. R. Stoyanov, J. M. Villegas, A. J. Cruz, L. L. Lockyear, J. H. Reibenspies, and D. P. Rillema, *Journal of Chemical Theory and Computation*, 2005, **1**, 95-106.
- 68 J. M. Villegas, S. R. Stoyanov, W. Huang, and D. P. Rillema, *Inorg. Chem.*, 2005, **44**, 2297-2309.
- 69 N. M. O'Boyle, A. L. Tenderholt, and K. M. Langner, *J. Comput. Chem.*, 2008, **29**, 839-845.
- 70 M. Headgordon, A. M. Grana, D. Maurice, and C. A. White, *J. Phys. Chem.*, 1995, **99**, 14261-14270.
- 71 W. R. Browne, N. M. O'Boyle, J. J. McGarvey, and J. G. Vos, *Chem. Soc. Rev.*, 2005, **34**, 641-663.

- 72 A. D. Becke, *J. Chem. Phys.*, 1993, **98**, 5648-5652.
- 73 C. Lee, W. Yang, and R. G. Parr, *Phys. Rev. B: Condens. Matter*, 1988, **37**, 785-789.
- 74 P. J. Hay and W. R. Wadt, *J. Chem. Phys.*, 1985, **82**, 270-283.
- 75 A. McLean, *J. Chem. Phys.*, 1980, **72**, 5639.